PHYSICAL REVIEW D VOLUME 7, NUMBER 4 15 FEBRUARY 1973

Polarization of Synchrotron Radiation from Relativistic Schwarzschild Circular Geodesics*

R. A. Breuer†
University of Maryland, College Park, Maryland 20742

and

C. V. Vishveshwara‡
New York University, New York, New York 10003
(Received 2 June 1972)

The pattern of geodesic synchrotron radiation emitted by a charge in an orbit close to the circular photon orbit at $3M$ around a nonrotating black hole of mass M is studied. The analysis is carried out using Stokes parameters, which completely characterize the state of the wave. The linear polarization, as observed at infinity, is total in the orbital plane and not smaller than 90% at the half-width of the beam. At the poles, pure circular polarization would be observed. In the region between the orbit plane and the poles the polarization shows features not present in ordinary synchrotron radiation. In our model, parameters more sensitive to deviations from the orbital plane are the Stokes parameter s_2 and the tilt angle of the polarization ellipse.

I. INTRODUCTION

Recently Misner *et al.*[1] showed that the generation of geodesic synchrotron radiation (GSR) in a curved background geometry of space-time is possible using Einstein's theory of general relativity. GSR is characterized by two conditions: (i) It is beamed into narrow equatorial angles, and (ii) the radiated frequencies are high harmonics of the particle's orbital frequency. Radiation modes with these two properties we henceforth call "synchrotron modes." Furthermore, the phenomenon of a "searchlight effect" appears in GSR as in ordinary synchrotron radiation.[2] The existence of scalar GSR was demonstrated for a test particle moving relativistically toward a nonrotating (Schwarzschild) black hole with the right impact parameter to approach the null circular geodesic orbit at $r=3M$. This large-angle scattering orbit (scattering angle $\gg 2\pi$) is approximated by a highly relativistic (unstable) circular particle orbit at $r_0=(3+\delta)M$ with the orbital frequency $\omega_0=(M/r_0^3)^{1/2}$. The radiated frequencies are limited by an exponential cutoff at $\omega_{\text{crit}}=m_{\text{crit}}\omega_0=(4/\pi\delta)\omega_0$ and related to the half-width of the beam $\Delta\vartheta$ for GSR for each harmonic number m by

$$\omega=m\omega_0, \quad \Delta\vartheta=|m|^{-1/2}. \tag{1.1}$$

Here $\vartheta\equiv\frac{1}{2}\pi-\theta$ is the latitude angle measured from the plane of the orbit. As $r_0\to 3M$, the width of the beam $\Delta\vartheta\to 0$; the radiation is confined to the equatorial plane.

A previous paper by Breuer, Ruffini, Tiomno, and Vishveshwara[3] shows a comparison of total power spectra of scalar, vector, and tensor GSR. The power distribution most like that of ordinary synchrotron radiation is that of a test particle coupling to a scalar field; here essentially all power is radiated into synchrotron modes. For nongeodesic (accelerated) circular orbits the scalar power spectrum $P_{\text{accel}}(\omega)$ is even more like the ordinary synchrotron one. For high frequencies ($\omega>\omega_{\text{crit}}$) Moncrief[4] obtains

$$P_{\text{accel}}(\omega)\simeq\frac{f^2}{\sqrt{4\pi}}\left(1-\frac{2M}{r_0}\right)^{1/4}\omega_0^2 \times 3\gamma\left(\frac{\omega}{\omega_{\text{crit}}}\right)^{1/2} \times\exp\left[-\frac{2\omega/\omega_{\text{crit}}}{(1-2M/r_0)^{1/2}}\right], \tag{1.2}$$

with f the scalar charge and $\omega_{\text{crit}}=3\gamma^3\omega_0$. This reduces to the electromagnetic synchrotron spectrum in the limit $M\to 0$.

As stated in Ref. 3, the shape for the scalar ($s=0$), vector ($s=1$), and tensor ($s=2$) spectra of GSR can approximately be summarized by

$$P\propto\omega^{1-s}\exp(-2\omega/\omega_{\text{crit}}).$$

The spectra broaden as s increases. The tensor radiation spectrum of circular geodesics is dominated by the $1/m$ dependence below the exponential cutoff; thus, compared with the scalar and vector cases, synchrotron modes in a very broad range of frequencies are excited, and low-frequency, wide-angle modes also carry a fraction of the energy.

Now we will consider the polarization properties of electromagnetic radiation as emitted by a charge moving under the same conditions as the particle described above. The inhomogeneous Maxwell equations for a point charge in arbitrary motion were obtained by Ruffini, Tiomno, and Vishveshwara.[5] Using their separation, we first solve the radial equations (Sec. II), obtain the relevant field quantities, and present the polarization properties in terms of the Stokes parameters (Sec. III). In the last section possible improvements and applications of a model for GSR are discussed.

II. THE RADIAL EQUATIONS

For the purpose of separating the inhomogeneous Maxwell equations (comma denotes partial derivative)

$$\frac{1}{\sqrt{-g}}(\sqrt{-g}F^{\mu\nu})_{,\nu}=j^{\mu}, \tag{2.1}$$

($F_{\mu\nu}=2A_{[\nu,\mu]}$ and $g=\det g_{\mu\nu}$), the electromagnetic field as well as its source is expanded in terms of vector spherical harmonics with odd parity $(-1)^{l+1}$ (magnetic) and even parity $(-1)^{l}$ (electric), where l is the angular momentum quantum number. After separation, one is left with two radial equations, one containing the even and the other the odd part of the source. Except for the source terms, the corresponding radial functions $a_{lm}(r,t)$, $b_{lm}(r,t)$ obey the same Schrödinger-type wave equation. In the vacuum case they satisfy the equation given by Wheeler.[6] Each Fourier component of our particular source varies harmonically and can be assumed to have the time dependence $\exp(-im\omega_0 t)$. Using the Regge-Wheeler coordinate $r^*=r-3M+2M\ln(rM^{-1}-2)$ instead of the Schwarzschild coordinate r, and for the current of a source with charge q

$$j^{\mu}=\frac{q}{\sqrt{-g}}\frac{dz^{\mu}}{dt}(1-2M/r)\times\delta(\theta-\tfrac{1}{2}\pi)\delta(\varphi-\omega_0 t)\delta(r^*-r_0{}^*), \tag{2.2}$$

we can write the odd and the even radial equations in the form

$$\frac{d^2a_{lm}}{dr^{*2}}+\left[m^2\omega_0{}^2-\left(1-\frac{2M}{r}\right)\frac{l(l+1)}{r^2}\right]a_{lm}=C_{lm}^{\text{odd}}\,\delta(r^*-r_0^*), \tag{2.3a}$$

$$\frac{d^2b_{lm}}{dr^{*2}}+\left[m^2\omega_0{}^2-\left(1-\frac{2M}{r}\right)\frac{l(l+1)}{r^2}\right]b_{lm}=C_{lm}^{\text{even}}\,\delta(r^*-r_0{}^*)_{,r^*}, \tag{2.3b}$$

where the coefficients are given by

$$C_{lm}^{\text{odd}}=\frac{q\omega_0}{l(l+1)}Y_{l,\theta}^{*m}(\tfrac{1}{2}\pi,0),\qquad C_{lm}^{\text{even}}=-\frac{q}{l(l+1)}Y_l^{*m}(\tfrac{1}{2}\pi,0). \tag{2.4}$$

The potential appearing in (2.1) and (2.2) differs from the scalar and tensor (odd and even) potentials by terms of $O(l^0)$ at most. The method of solving (2.3a) is outlined in Misner et al.[1] and discussed in detail by Breuer et al.[7] It uses basically Green's functions, obtained by matching solutions L and R of the homogeneous equations at $r^*=r_0^*$. $L(r^*)$ represents a scattering wave function with an incident wave moving to the left, and similarly $R(r^*)$ represents a scattering wave function with the incident wave moving to the right. The Green's function $G(r^*,r_0^*)$ which is a solution of

$$-\frac{d^2G}{dr^{*2}}+[V-m^2\omega_0{}^2]G=\delta(r^*-r_0^*) \tag{2.5}$$

assumes the following special forms for the various source terms in (2.3). For Eq. (2.3a)

$$G(r^*,r_0^*)=\begin{cases}\dfrac{i}{2\mathcal{T}}L(r_0^*)R(r^*), & r^*>r_0^*\\[2mm] \dfrac{i}{2\mathcal{T}}R(r_0^*)L(r^*), & r^*\leq r_0^*\end{cases} \tag{2.6a}$$

where $\mathcal{T}$ is the transmission amplitude, and for Eq. (2.3b)

$$G'(r^*,r_0^*)=\begin{cases}\dfrac{i}{2\mathcal{T}}L'(r_0^*)R(r^*), & r^*>r_0^*\\[2mm] \dfrac{i}{2\mathcal{T}}R'(r_0^*)L(r^*), & r^*\leq r_0^*\end{cases} \tag{2.6b}$$

where $G'\equiv\partial G/\partial r_0^*$. The complete solutions of Eqs. (2.3) are then

$$a_{lm}(r^*,t)=-C_{lm}^{\text{odd}}\frac{i}{2(m\omega_0)^{1/2}}L(r_0^*)e^{im\omega_0(r^*-t)}, \tag{2.7a}$$

$$b_{lm}(r^*,t)=C_{lm}^{\text{even}}\frac{i}{2(m\omega_0)^{1/2}}L'(r_0^*)e^{im\omega_0(r^*-t)} \tag{2.7b}$$

at large r^*, where $R(r^*)\sim(m\omega_0)^{-1}\mathcal{T}\exp(im\omega_0 r^*)$. For the synchrotron modes ($m\gg1$) the parabolic WKB method gives the wave function in terms of parabolic cylinder functions, $L(r^*)\propto D_{-1/2-i\epsilon/2}(-z)$ and $R(r^*)\propto D_{-1/2-i\epsilon/2}(+z)$, with $z=(1-i)[l(l+1)]^{1/4}\times(3M)^{-1}r^*$, which can be converted into Γ functions in the limit $r_0^*=3M\delta\to0$. The ϵ's are the barrier integrals as evaluated in Misner et al.[1]: $\epsilon=1+2l-2|m|+|m|\delta$. We use the notation for the even and odd parity as in Ref. 3:

$$\epsilon_{\text{odd}}=3+4p+|m|\delta=3+4p+\frac{4}{\pi}\frac{\omega}{\omega_{\text{crit}}},\qquad l-|m|=2p+1$$

$$\epsilon_{\text{even}}=1+4q+|m|\delta+1+4q+\frac{4}{\pi}\frac{\omega}{\omega_{\text{crit}}},\qquad l-|m|=2q \tag{2.8}$$

with p and q integers. The definition of ω_{crit} is the same as in the scalar case:

$$\frac{\omega_{\text{crit}}}{\omega_0}=m_{\text{crit}}=\frac{12}{\pi}\gamma^2\,. \tag{2.9}$$

Having obtained the solutions (2.7) for the radial functions, we are now able to calculate the components of the electric field.

III. POLARIZATION AND STOKES PARAMETERS

In order to study the radiation properties as observed at infinity, we must know the asymptotic behavior of the electric field $E^i \equiv F^{0i}$. The physically meaningful components are the E_i, when evaluated in a locally orthonormal frame:

$$F_{\hat\alpha\hat\beta}=F_{\mu\nu}\omega^{\mu}_{\hat\alpha}\omega^{\nu}_{\hat\beta}\,, \tag{3.1}$$

where the orthonormal tetrad field is defined by

$$\begin{aligned}
\omega^{\mu}_{\hat t}&=(1-2Mr^{-1})\delta^{\mu}_{0}\,,\\
\omega^{\mu}_{\hat r}&=(1-2Mr^{-1})^{-1}\delta^{\mu}_{r}\,,\\
\omega^{\mu}_{\hat\theta}&=r^{-1}\delta^{\mu}_{\theta}\,,\\
\omega^{\mu}_{\hat\varphi}&=(r\sin\theta)^{-1}\delta^{\mu}_{\varphi}\,.
\end{aligned} \tag{3.2}$$

The field components determining the radiation at $r\to\infty$ are then

$$\begin{aligned}
E^{\text{odd}}_{\hat\theta}&=-\sum\frac{im\omega_0}{r}a_{lm}\frac{1}{\sin\theta}Y^m_{l,\varphi}\,,\\
E^{\text{odd}}_{\hat\varphi}&=\sum\frac{im\omega_0}{r}a_{lm}Y^m_{l,\theta}\,,\\
E^{\text{even}}_{\hat\theta}&=\sum\frac{im\omega_0}{r}b_{lm}Y^m_{l,\theta}\,,\\
E^{\text{even}}_{\hat\varphi}&=\sum\frac{im\omega_0}{r}b_{lm}\frac{1}{\sin\theta}Y^m_{l,\varphi}\,.
\end{aligned} \tag{3.3}$$

The summation includes all terms for which $l \geq |m|$. The longitudinal fields do not contain radiation terms such as $E^{\text{odd}}_{\hat r}=0$ and $E^{\text{even}}_{\hat r}\sim r^{-2}$. The radiation per solid angle splits naturally into two parts, one in the θ direction and one in the φ direction; the respective intensities are called the "vertical" and the "horizontal" polarizations, $J_\perp$ and $J_\parallel$:

$$\begin{aligned}
J_\perp&=|E^{\text{odd}}_{\hat\theta}+E^{\text{even}}_{\hat\theta}|^2\,,\\
J_\parallel&=|E^{\text{odd}}_{\hat\varphi}+E^{\text{even}}_{\hat\varphi}|^2\,,
\end{aligned} \tag{3.4}$$

a characterization suggestive of an observer in the equatorial plane. The sum of both gives us the total power per unit solid angle,

$$\frac{dP(\omega)}{d\Omega}=J_\perp+J_\parallel\,, \tag{3.5}$$

which is plotted in Fig. 1. As modes with $l>|m|+1$

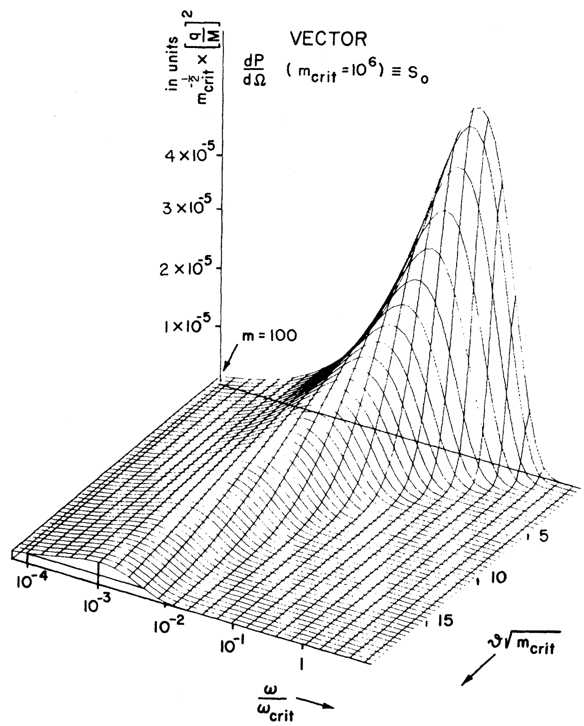

FIG. 1. Power per unit solid angle or Stokes parameter S_0. $\vartheta\equiv\frac{1}{2}\pi-\theta$, where θ is the polar angle. The ϑ axis is chosen so that the half-width of the beam is at $\vartheta\sqrt{m_{\text{crit}}}=1$ for $\omega/\omega_{\text{crit}}=1$. Although computed for $m_{\text{crit}}=10^6$, corrections to this plot for other values of m_{crit} are of order $(m/m_{\text{crit}})^{1/2}$.

add less than 2% to the power at the peak ($l=|m|$ in the even, $l=|m|+1$ in the odd case), all quantities can be evaluated in the "sychrotron approximation," defined by

$$\begin{aligned}
&|m|\gg 1\,,\\
&\frac{p}{|m|},\ \frac{q}{|m|}\ll 1\,.
\end{aligned} \tag{3.6}$$

The explicit formulas for both the field components and (3.3), and the total power per solid angle (3.5) using the synchrotron approximation, are derived in the Appendix. Equation (3.5) is of the form

$$\begin{aligned}
\frac{dP}{d\Omega}=C\Big[&(m^{3/2}C_1+m^{1/2}C_2+mC_3)\sin^2\vartheta\\
&+m^{3/2}C_1\left(\sin^2\vartheta-\frac{1}{m}\cos^2\vartheta\right)^2+m^{1/2}C_2\\
&+mC_3\left(\sin^2\vartheta-\frac{1}{m}\cos^2\vartheta\right)\Big]\,,
\end{aligned} \tag{3.7}$$

where the coefficient $C\propto\cos^{2m-2}\vartheta$ and C_1, C_2, C_3 (not to be confused with the C_{lm}) contain functions with complex arguments involving m/m_{crit} (see Appendix). C_1 and C_2 are the factors coupled to the odd and even modes, respectively, while C_3 multiplies the contribution due to the interaction term of the two modes. Figure 1 shows a strong confinement of the power in a range of one decade around $\omega \simeq 0.25\omega_{crit}$, which is $m\delta \simeq 0.2$. The angular dependence of $dP/d\Omega$ exhibits the increasing beaming feature with increasing frequency. To study the behavior of the individual even or odd modes, one sets $C_2, C_3 = 0$ in (3.6) to get the odd mode, or C_1, $C_3 = 0$ to get the even mode. For these cases we find the following ratio of perpendicular to total power per unit solid angle.

$$\text{odd: } \frac{J_\perp}{J_\parallel + J_\perp} = \frac{\sin^2\vartheta}{1+\sin^2\vartheta}, \tag{3.8a}$$

$$\text{even: } \frac{J_\perp}{J_\parallel + J_\perp} = \frac{\sin^2\vartheta}{\sin^2\vartheta + [\sin^2\vartheta - (1/m)\cos^2\vartheta]^2}. \tag{3.8b}$$

However, as mentioned in Ref. 3, the contribution of the odd modes to the total (integrated) power $P = \int d\Omega(dP/d\Omega)$ is always less by two orders of magnitude than that of the even modes.

The polarization state of a wave with two degrees of freedom, together with its intensity, is completely characterized by Stokes parameters.[8] If the amplitudes are, as in our case, $E_{\hat\theta}$ and $E_{\hat\varphi}$, the polarization matrix ρ can be written as $(i, j = \hat\theta, \hat\varphi)$

$$\begin{aligned}\rho &= (E_i^* E_j) \\ &= \tfrac{1}{2}\sum_{\mu=0}^{3} S_\mu \sigma_\mu \\ &= \tfrac{1}{2}(S_0 \cdot 1 + \vec{S}\cdot\vec{\sigma}) \\ &= \begin{pmatrix} |E_{\hat\theta}|^2 & E_{\hat\theta}E_{\hat\varphi}^* \\ E_{\hat\theta}^* E_{\hat\varphi} & |E_{\hat\varphi}|^2 \end{pmatrix}. \end{aligned} \tag{3.9}$$

The four σ_μ are the usual two-dimensional Pauli spin matrices. The Stokes parameters S_μ can be written as $S_\mu = \mathrm{trace}(\rho\sigma_\mu)$, namely

$$\begin{aligned} S_0 &= |E_{\hat\theta}|^2 + |E_{\hat\varphi}|^2 = J_\parallel + J_\perp \equiv \frac{dP}{d\Omega}, \\ S_1 &= |E_{\hat\theta}|^2 - |E_{\hat\varphi}|^2 = J_\parallel - J_\perp, \\ S_2 &= E_{\hat\theta}E_{\hat\varphi}^* + E_{\hat\theta}^* E_{\hat\varphi}, \\ S_3 &= +i(E_{\hat\theta}E_{\hat\varphi}^* - E_{\hat\theta}^* E_{\hat\varphi}), \end{aligned} \tag{3.10}$$

where S_0 is the total power per unit solid angle, plotted in Fig. 1. S_1 represents the difference of the θ and φ power components. S_2 and S_3 are complementary to each other, as are S_0 and S_1. While S_1 is proportional to the real part of the cross correlation of $E_{\hat\theta}$ and $E_{\hat\varphi}$, S_2 is proportional to its imaginary part.

The description of a plane wave of given frequency by these parameters is complete in the sense that if two waves have identical S_μ, then the waves are identical up to a phase factor. S_1, S_2, and S_3 determine the state of polarization. For that purpose it is convenient to introduce the normalized Stokes parameters

$$s_0 = 1, \quad s_1 = S_1/S_0, \quad s_2 = S_2/S_0, \quad s_3 = S_3/S_0 \tag{3.11}$$

and define the degrees of linear and circular polarization d_L and d_C by

$$d_L = (s_1^2 + s_2^2)^{1/2}, \quad d_C = |s_3|. \tag{3.12}$$

Consequently, the "degree of polarization" d, defined as the ratio of the completely polarized power to the total power, must be

$$d = (s_1^2 + s_2^2 + s_3^2)^{1/2} = (d_L^2 + d_C^2)^{1/2}, \tag{3.13}$$

which is unity for a totally polarized wave. For any coherent sources such as the circular orbit assumed in this paper, one of course has $d = 1$. The Stokes parameters are explicitly derived in the Appendix, and in their normalized form together with the degree of linear and circular polarization they are sketched in the Figs. 2–5. s_2 changes more rapidly than any other parameter. An observer at infinity would see 100% linear or 100% circular polarization if located in the orbital plane or near the direction of the poles, respectively. This feature holds as in ordinary synchrotron radiation. Between the plane of the orbit and the poles, waves generally are elliptically polarized. The increase of ellipticity, however, is different for GSR from the ordinary case.[9] One observes a characteristic maximum at an angle ϑ_0 in d_C or s_2, corresponding to a minimum in d_L or a zero in s_1. From $s_1 = 0$ or $J_\parallel - J_\perp = 0$ one finds that in the range of interest ($m \gg 1$; therefore $\vartheta \ll 1$) with $\Delta\vartheta = |m|^{-1/2}$ approximately (see, e.g., Fig. 2)

$$\vartheta_0 \simeq 3 \times \Delta\vartheta = 3 \times \text{beam half-width}. \tag{3.14}$$

In this limit this relation is independent of m. The inclination of the polarization ellipse defines some angle τ between its major axis and the orbit plane, the "tilt angle of the polarization ellipse." One gets $\tau = 0$ for horizontal and $\tau = \frac{1}{2}\pi$ for vertical polarization. The ratio of the two axes of the polarization ellipse defines an angle ϵ by[8]

$$\pm\frac{\text{major axis}}{\text{minor axis}} = \cot\epsilon, \quad -\tfrac{1}{4}\pi < \epsilon < \tfrac{1}{4}\pi \tag{3.15}$$

where the minus sign stands for right-handed and the plus sign for left-handed polarization.[10] The relations between τ, ϵ, and the Stokes parameters are

$$\tau = -\tfrac{1}{4} i \ln \frac{s_1^2 - s_2^2 + 2is_1 s_2}{s_1^2 + s_2^2}, \tag{3.16}$$

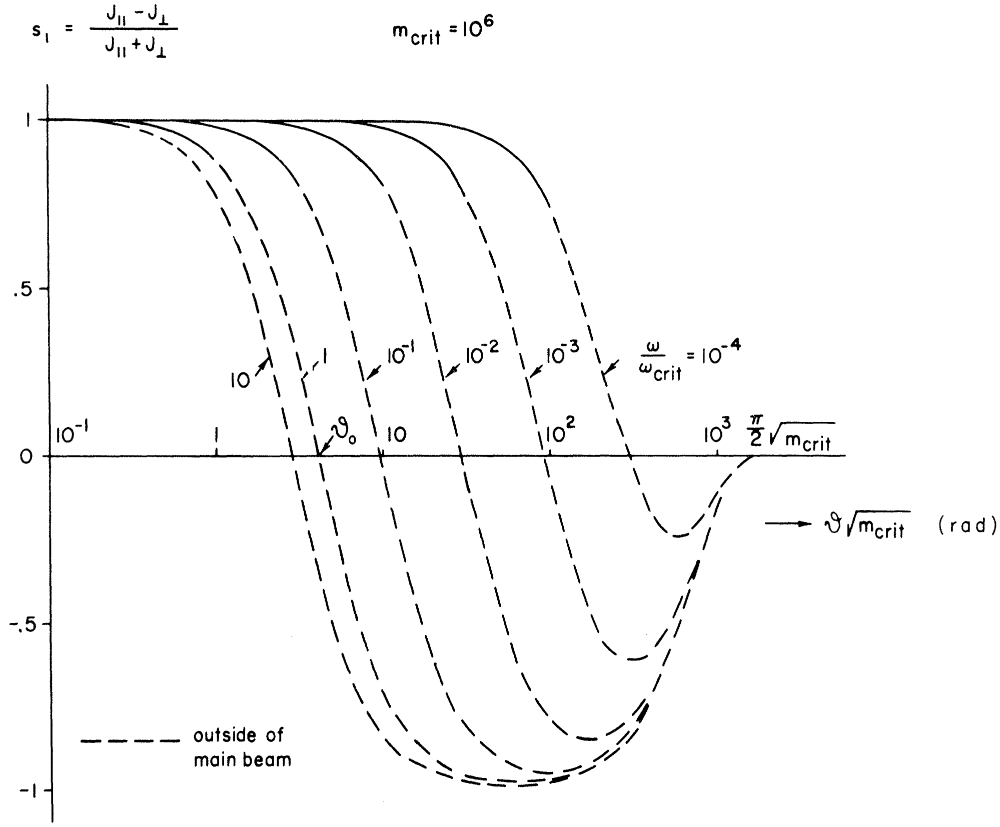

FIG. 2. Normalized Stokes parameter s_1. The angle ranges logarithmically from the orbital plane to the (north) pole. These curves and those of Figs. 3 – 6 are independent of m_{crit} when $m >> 1$ and $\vartheta\sqrt{m_{crit}} \lesssim 10$.

$$\epsilon = -\tfrac{1}{2} i \ln[(d_L - i s_3)/d], \qquad (3.17)$$

with the same sign convention as in (3.15). One gets $\epsilon = \pm\frac{1}{4}\pi$ for left- and right-handed circular polarization, respectively, while $\epsilon = 0$ for pure linear polarization.

The waves above the orbital plane are generally right elliptically polarized and tend towards right circular polarization at the north pole. Simultaneously, as can be seen from Fig. 6, the polarization ellipse undergoes a monotonic change from horizontal to vertical polarization. At negative latitude $\vartheta < 0$ the waves would be left elliptically polarized. One notices the different sensitivity of the parameters to a small increase in the latitude. Unlike d_L, which does not drop below 90% for the peak harmonics within the main beam, one gets $\tau \simeq 15°$, $d_C \simeq 25\%$, and $s_2 \simeq 40\%$ at the half-width of the beam; at ϑ_0 we even have $s_1 = 0$, $s_2 \simeq 85\%$, $d_C \simeq 50\%$ and $\tau = \frac{1}{4}\pi$.

IV. DISCUSSION

In the foregoing we have studied in detail the polarization of electromagnetic synchrotron radiation We can, however, expect the corresponding properties of tensor radiation, which we are presently investigating, to exhibit similar features[11,18] so that the discussion to follow is valid.

Although we are dealing with a model for GSR which is astrophysically unrealistic because the orbits invoked are unstable, it nevertheless is desirable to study the polarization properties as a setting-up exercise preparatory to searches for more plausible sources of GSR. Any other model will only be acceptable in connection with Weber's observations[12] if it still distinguishes the galactic plane, as does a recent one suggested by Penrose[13] involving naked singularities in the center of the galaxy. Mainly, the assumption of isotropic radiation had led Weber to an estimate of the annual mass loss for our galaxy, which would mean that the present evolutionary epoch is special. At present, only extremely anisotropic radiation seems compatible with the lower mass-loss-rate estimates for the galaxy on the basis of the radiation measured by Weber's gravity telescope and the upper limit placed by galactic dynamics on the mass-loss rate. A mass-loss rate of more than $200 M_\odot$/yr

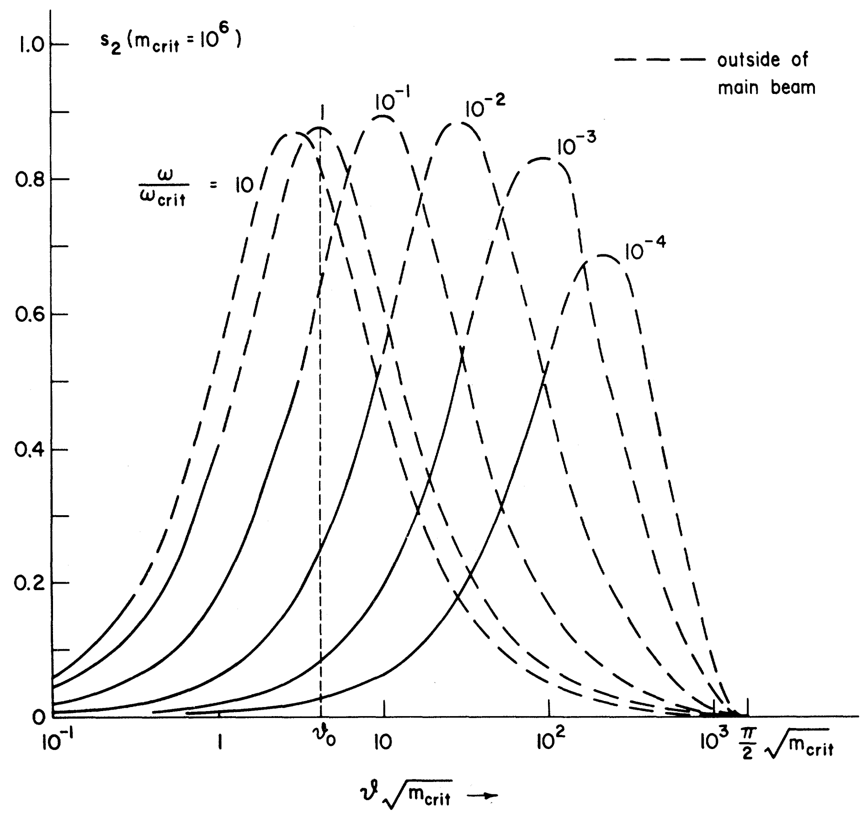

FIG. 3. Normalized Stokes parameter s_2.

would be inconsistent with observations of stellar orbits.[14] For any radiation with only moderate anisotropy one can extrapolate to a loss rate of 10^3 solar masses per year, but also, with different assumptions on the efficiency of the gravity telescope and the bandwidth of the signals, one can arrive at numbers like $3\times10^6 M_\odot$/yr, as was done by Kafka.[15] Secondly, frequency multiplication should take place with high harmonics of mechanical motion frequencies present, so kilocycle frequencies can be emitted by coherent sources much more massive than a few solar masses.

Radiation from particles in the galactic plane would lead one to expect a strong linear polarization, as confirmed by the present calculation: The earth's position with respect to the galactic plane is $z_\odot = (4 \pm 12)$ parsec; if we place the earth not exactly in the plane but at $\Delta\vartheta = 10^{-3}$ rad and identify this angle with the beam half-width ($m = 10^6$ from $\Delta\vartheta = |m|^{-1/2}$), the degree of linear polarization d_L is above 90% (100% in the plane itself) and the Stokes parameter s_1 is still above 85%. But as Tyson and Douglass[16] have pointed out, Weber's data are not consistent with a high degree of s_1 (what they call "degree of linear polarization"), assuming the source is located at the center of the galaxy. The upper limit they impose on s_1 is 40%.

What therefore have to be changed in the present model are the related properties of the source motion and the polarization of the radiation produced. Of course, artificial orbits have to be avoided. One has to allow the possibility of the production of highly anisotropic radiation which is unpolarized when averaged over many pulses.

If one actually had a polarized source (which could still be true for the single events), then the tilt angle of the polarization ellipse and the Stokes parameter s_2 would be highly sensitive to deviations from the galactic plane; they show strong dependence on the polar angle. Measurable quantities varying rapidly with small changes in the latitude are the appropriate discriminants needed for determining the earth's location. One is indeed able to redefine the Stokes parameters for gravitational waves.[17] The parameters s_1 and s_2, then related to the linear polarization of tensor waves, can be measured by the gravity telescopes of Weber and of Tyson and Douglass (to obtain s_2 the instrument has to be rotated by $\frac{1}{8}\pi$ with respect to the position which measures s_1). If synchrotron modes of gravitational radiation are being detected – with the proviso that a different source mechanism is gen-

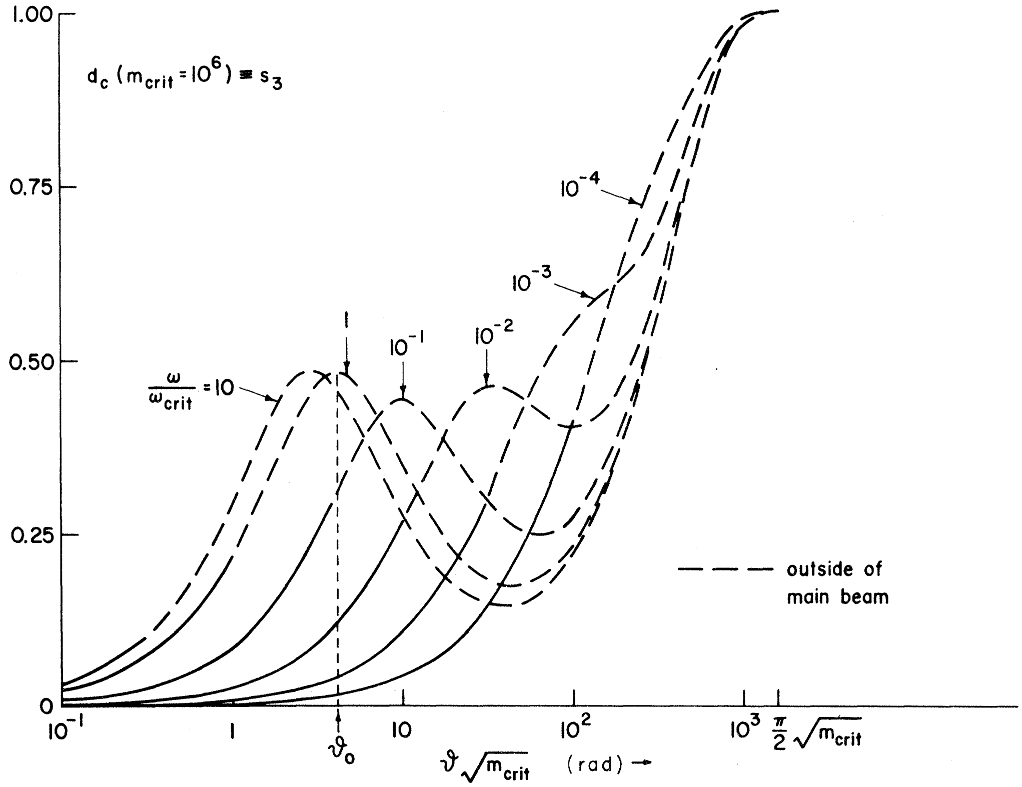

FIG. 4. Degree of circular polarization or normalized Stokes parameter $|s_3|$. For positive latitudes ϑ, i.e., above the orbit plane (in the sense of the orbital angular momentum) the waves are right elliptically polarized.

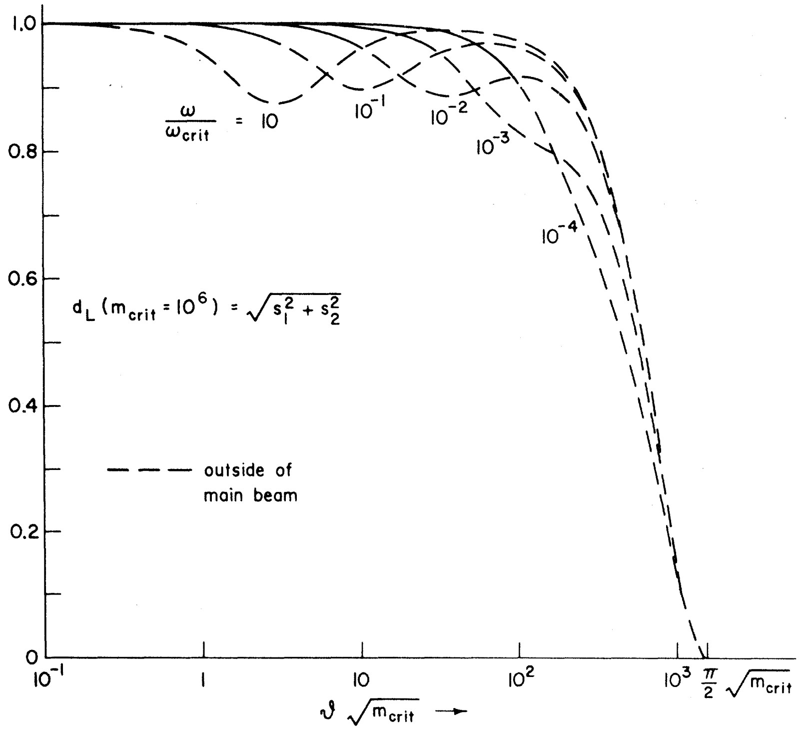

FIG. 5. Degree of linear polarization. The radiation is completely polarized; therefore $d_L{}^2 + d_C{}^2 = 1$ at all angles and frequencies.

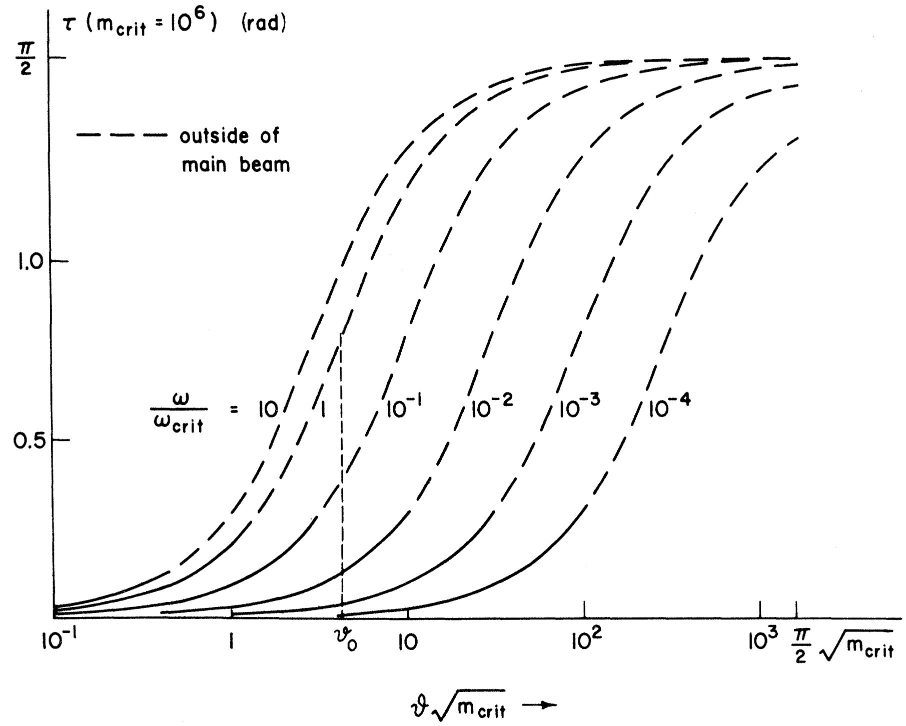

FIG. 6. Tilt angle of the polarization ellipse. τ is the angle enclosed by the major axis of the ellipse and the orbital plane and is an odd function of ϑ. At ϑ_0 the tilt angle is 45° for all frequencies with $m \gg 1$.

erating them – we expect that the possibility exists to measure the latitude of the earth more accurately.

ACKNOWLEDGMENTS

We want to express our thanks to Professor C. W. Misner for many fruitful discussions and constant encouragement. We also would like to thank Professor D. R. Brill, P. L. Chrzanowski, L. G. Fishbone, and H. G. Hughes III for helpful conversations. The assistance of R. L. Tobias with some of the numerical calculations is very much appreciated.

APPENDIX

To apply the synchrotron approximation (3.6) to the electric field components (3.3) we need the asymptotic forms for the coefficients appearing in the source equation (2.3) and for the vector spherical harmonics. The synchrotron approximation sets $p, q = 0$ in (2.8) and $m \gg 1$. Using Sterling's formula we get (up to order m^{-2})

$$C^{\text{odd}}_{m+1,m} = q\omega_0(-)^{m+1}\pi^{-3/4}m^{-5/4}(1-13/8m), \tag{A1a}$$

$$C^{\text{even}}_{m,m} = q(-)^{m+1}(4\pi^3)^{-1/4}m^{-7/4}(1-3/4m). \tag{A1b}$$

In this limit the components of the vector spherical harmonics are

$$\begin{aligned}
&\frac{1}{\sin\theta}Y^m_{m+1,\varphi} = i(-)^m\pi^{-3/4}m^{7/4}(1+11/8m)\cos\theta\sin^{m-1}\theta\, e^{im\varphi},\\
&\sin\theta\, Y^m_{m+1,\theta} = (-)^m\pi^{-3/4}m^{7/4}(1+11/8m)\left(\cos^2\theta - \frac{1}{m}\sin^2\theta\right)\sin^m\theta\, e^{im\varphi},\\
&Y^m_{m,\theta} = (-)^m(4\pi^3)^{-1/4}m^{5/4}(1+1/4m)\cos\theta\sin^{m-1}\theta\, e^{im\varphi},\\
&Y^m_{m,\varphi} = i(-)^m(4\pi^3)^{-1/4}m^{5/4}(1+1/4m)\sin^m\theta\, e^{im\varphi}.
\end{aligned} \tag{A2}$$

In order to obtain the approximation $\epsilon \gg 1$, valid in the region of exponential cutoff, for the various field amplitudes, we will use the following asymptotic expressions for the Γ functions:

$$\Gamma(\tfrac{1}{4}+\tfrac{1}{4}i\epsilon_{\text{odd}}) \simeq \sqrt{2\pi}\,(4/\epsilon_{\text{odd}})^{1/4} \exp\{\tfrac{1}{4}i[\epsilon_{\text{odd}} \ln(\tfrac{1}{4}\epsilon_{\text{odd}}) - \tfrac{1}{2}\pi - \epsilon_{\text{odd}}] - \tfrac{1}{8}\pi\epsilon_{\text{odd}}\}$$
$$\Gamma(\tfrac{3}{4}+\tfrac{1}{4}i\epsilon_{\text{even}}) \simeq \sqrt{2\pi}(\tfrac{1}{4}\epsilon_{\text{even}})^{1/4} \exp\{\tfrac{1}{4}i[\epsilon_{\text{even}} \ln(\tfrac{1}{4}\epsilon_{\text{even}}) + \tfrac{1}{2}\pi - \epsilon_{\text{even}}] - \tfrac{1}{8}\pi\epsilon_{\text{even}}\}. \tag{A3}$$

Substituting these values back into (3.3), and using the asymptotic forms for $L(r_0^*)$ and $L'(r_0^*)$ given in Breuer *et al.*,[7] one gets immediately in the synchrotron approximation and the $\epsilon \gg 1$ limit, respectively,

$$E_{\hat\theta}^{\text{odd}} = -iq\omega_0^{3/2}(27)^{1/4}e^{-i\pi/8}(4\pi^2 r)^{-1}m^{3/4}(1-1/2m)e^{-\alpha_o - i\beta_o}\Gamma(\tfrac{1}{4}+\tfrac{1}{4}i\epsilon_{\text{odd}})\cos\theta\, f(\theta,\varphi,t) + O(m^{-2})$$
$$\simeq -iq\omega_0^{3/2}(27)^{1/4}[(3+m\delta)^{1/4}4\pi^{3/2}r]^{-1}m^{3/4}\exp[-2\alpha_o(1+i) - i\tfrac{1}{4}\pi]\cos\theta\, f(\theta,\varphi,t) + O(m^{-1}) \quad (\epsilon \gg 1)$$
$$E_{\hat\theta}^{\text{even}} = \frac{(i-1)}{r}\omega_0^{1/2}qe^{-i\pi/8}(32\pi^4\sqrt{27})^{-1/2}m^{1/4}(1-1/2m)e^{-\alpha_e - i\beta_e}\Gamma(\tfrac{3}{4}+\tfrac{1}{4}i\epsilon_{\text{even}})\cos\theta\, f(\theta,\varphi,t)$$
$$\simeq \frac{(i-1)\omega_0^{1/2}q}{(32\pi^3\sqrt{27})^{1/2}r}(1+m\delta)^{1/2}e^{-2\alpha_e(1+i)}m^{1/4}\cos\theta\, f(\theta,\varphi,t) \quad (\epsilon \gg 1) \tag{A4}$$
$$E_{\hat\varphi}^{\text{odd}} = q\omega_0^{3/2}(27)^{1/4}e^{-i\pi/8}m^{3/4}(1-1/2m)(4\pi^2 r)^{-1}e^{-\alpha_o - i\beta_o}\Gamma(\tfrac{1}{4}+\tfrac{1}{4}i\epsilon_{\text{odd}})[\cos^2\theta - (1/m)\sin^2\theta]f(\theta,\varphi,t) + O(m^{-2})$$
$$\simeq q\omega_0^{3/2}(27)^{1/4}[(3+m\delta)^{1/4}4\pi^{3/2}r]^{-1}m^{3/4}e^{-2\alpha_o(1+i) - i\pi/4}[\cos^2\theta - (1/m)\sin^2\theta]f(\theta,\varphi,t) + O(m^{-1}), \quad (\epsilon \gg 1)$$
$$E_{\hat\varphi}^{\text{even}} = -\frac{(1+i)}{r}\omega_0^{1/2}q\frac{e^{-i\pi/8}}{(\sqrt{27}\,32\pi^4)^{1/2}}m^{1/4}(1-1/2m)e^{-\alpha_e - i\beta_e}\Gamma(\tfrac{3}{4}+\tfrac{1}{4}i\epsilon_{\text{even}})f(\theta,\varphi,t)$$
$$\simeq -\frac{(1+i)}{r}\omega_0^{1/2}q(32\pi^3\sqrt{27})^{-1/2}(1+m\delta)^{1/2}e^{-2\alpha_e(1+i)}m^{1/4}f(\theta,\varphi,t) \quad (\epsilon \gg 1).$$

Here we made use of the following abbreviations:

$$\alpha_o = \tfrac{1}{8}\pi\epsilon_{\text{odd}}, \quad \beta_o = \tfrac{1}{4}\epsilon_{\text{odd}}\ln(\tfrac{1}{4}\epsilon_{\text{odd}}),$$
$$\alpha_e = \tfrac{1}{8}\pi\epsilon_{\text{even}}, \quad \beta_e = \tfrac{1}{4}\epsilon_{\text{even}}\ln(\tfrac{1}{4}\epsilon_{\text{even}}),$$
$$f(\theta,\varphi,t) = \sin^{m-1}\theta\, e^{im\varphi}e^{im\omega_0(r^*-t)}. \tag{A5}$$

The power per solid angle (3.6) contains four coefficients: the over-all factor

$$C = \frac{q^2\omega_0}{16\pi^4 r^2\sqrt{27}}\cos^{2m-2}\vartheta\exp(-\tfrac{1}{2}\pi - m/m_{\text{crit}}), \tag{A6}$$

as well as C_1 for the odd mode, C_2 for the even mode, and C_3 for the interaction terms. The synchrotron approximation yields with the use of (A1)–(A4)

$$C_1 = e^{-\pi/4}(1+\tfrac{1}{3}\delta)^{-3}|\Gamma(\tfrac{1}{4}+\tfrac{1}{4}i\epsilon_{\text{odd}})|^2,$$
$$C_2 = e^{\pi/4}|\Gamma(\tfrac{3}{4}+\tfrac{1}{4}i\epsilon_{\text{even}})|^2,$$
$$C_3 = -(1+\tfrac{1}{3}\delta)^{-3/2}\{\exp[-i(\tfrac{1}{4}\pi - \ln 2 - \beta_e + \beta_o)]\Gamma(\tfrac{1}{4}+\tfrac{1}{4}i\epsilon_{\text{odd}})\Gamma^*(\tfrac{3}{4}+\tfrac{1}{4}i\epsilon_{\text{even}}) + \text{c.c.}\}. \tag{A7}$$

In the limit $\epsilon \gg 1$ (region of exponential cutoff in the power spectrum) (A7) reduces to

$$C_1 = e^{-\pi/2}(1+\tfrac{1}{3}\delta)^{-3}(3+m\delta)^{-1/2},$$
$$C_2 = \tfrac{1}{4}e^{\pi/2}(1+m\delta)^{1/2},$$
$$C_3 = (1+\tfrac{1}{3}\delta)^{-3/2}\sin(\tfrac{1}{2})\left(\frac{1+m\delta}{3+m\delta}\right)^{1/4}. \tag{A8}$$

At the peak of the spectrum ($m\delta = 1$, $\delta \ll 1$) their values are simply

$$C_1 = \tfrac{1}{2}e^{-\pi/2},$$
$$C_2 = \tfrac{1}{2}\sqrt{2}\,e^{\pi/2},$$
$$C_3 = 2^{-1/4}\sin(\tfrac{1}{2}). \tag{A9}$$

With the help of (A4), the Stokes parameters can now be evaluated according to formulas (3.9). While for S_1 only a minus sign has to be placed in front of the first term in (3.7), S_2 and S_3 yield to more complicated expressions:

$$S_2=\frac{q^2\omega_0^2\exp(-\alpha_o-\alpha_e)}{(4\pi^2r)^2}\cos^{2m}\vartheta\,\sin\vartheta\, m\{\exp[-i(\beta_e-\beta_o+\tfrac{1}{4}\pi)]\,\Gamma(\tfrac{3}{4}+\tfrac{1}{4}i\epsilon_{\text{even}})\Gamma^*(\tfrac{1}{4}+\tfrac{1}{4}i\epsilon_{\text{odd}})+\text{c.c}\}, \tag{A10}$$

$$S_3=\frac{2q^2\omega_0}{(4\pi^2r)^2\sqrt{27}}\cos^{2m-2}\vartheta\,\sin\vartheta\sqrt{m}\,\big(e^{-2\alpha_e}|\Gamma(\tfrac{3}{4}+\tfrac{1}{4}i\epsilon_{\text{even}})|^2+27\omega_0^2e^{-2\alpha_o}m|\Gamma(\tfrac{1}{4}+\tfrac{1}{4}i\epsilon_{\text{odd}})|^2[\sin^2\vartheta-(1/m)\cos^2\vartheta]$$
$$+\sqrt{27}\,\omega_0\exp(-\alpha_o-\alpha_e)\sqrt{m}\,[1+\sin^2\vartheta-(1/m)\cos^2\vartheta]\tfrac{1}{2}i$$
$$\times\{\exp[i(\beta_e-\beta_o+\tfrac{1}{4}\pi)]\Gamma(\tfrac{1}{4}+\tfrac{1}{4}i\epsilon_{\text{odd}})\Gamma^*(\tfrac{3}{4}+\tfrac{1}{4}i\epsilon_{\text{even}})-\text{c.c.}\}\big). \tag{A11}$$

*Supported in part by NASA Grant No. NGR-21-002-010 and NSF Grant No. GU-3186.

†Fellow of the German National Fellowship Foundation, Present address: Institut für Theoretische Physik, Röntgenring 8, 87 Würzburg, W. Germany.

‡Present address: Dept. of Physics, Boston University, Boston, Mass. 02215.

[1]C. W. Misner, R. A. Breuer, D. R. Brill, P. L. Chrzanowski, H. G. Hughes III, and C. M. Pereira, Phys. Rev. Letters 28, 998 (1972).

[2]H. G. Hughes III (unpublished).

[3]R. A. Breuer, R. Ruffini, J. Tiomno, and C. V. Vishveshwara, preceding paper, Phys. Rev. D 7, 1002 (1973).

[4]V. Moncrief (unpublished).

[5]R. Ruffini, J. Tiomno, and C. V. Vishveshwara, Lett. Nuovo Cimento 3, 211 (1971).

[6]J. A. Wheeler, in *Geometrodynamics* (Academic, New York, 1962), p. 203.

[7]R. A. Breuer, P. L. Chrzanowski, H. G. Hughes III, and C. W. Misner (unpublished).

[8]J. D. Kraus, *Radio Astronomy* (McGraw-Hill, New York, 1966).

[9]See e.g., A. A. Sokolov and I. M. Ternov, *Synchrotron Radiation* (Pergamon, New York, 1968).

[10]A wave is right circularly polarized when the electric field vector is rotating counterclockwise with the wave approaching or clockwise with the wave receding.

[11]See also D. M. Chitre and R. H. Price, Phys. Rev. Letters 29, 185 (1972).

[12]J. Weber, Phys. Rev. Letters 25, 180 (1970).

[13]R. Penrose, Sci. Am. 226, 38 (1972).

[14]D. W. Sciama, Nature 224, 1263 (1969).

[15]P. Kafka, Gravity Essay, 1972 (unpublished).

[16]J. A. Tyson and D. H. Douglass, Phys. Rev. Letters 28, 994 (1972); and private communication.

[17]R. A. Breuer (unpublished).

[18]R. A. Breuer, J. Tiomno, and C. V. Vishveshwara, Lett. Nuovo Cimento 4, 857 (1972).